Preprints (www.preprints.org) | NOT PEER-REVIEWED | Posted: 4 April 2017 doi:10.20944/preprints201704.0018.v1

Peer-reviewed version available at Nanomaterials 2017, 7, , 129; doi:10.3390/nano7060129

Article

Development of Non-Enzymatic Glucose Biosensors Based on Electrochemically Prepared Polypyrrole-Chitosan-Titanium Dioxide Nanocomposite Films

Ali M.A. Abdul Amir AL-Mokaram [1,2,*], Rosiyah Yahya [1], Mahnaz M. Abdi [3,4] and Habibun Nabi Muhammad Ekramul Mahmud [1,*]

[1] Department of Chemistry, Faculty of Science, University of Malaya, 50603, Kuala Lumpur, Malaysia; rosiyah@um.edu.my
[2] Department of Chemistry, College of Science, Al-Mustansiriya University, 10052- Baghdad, Iraq
[3] Department of Chemistry, Faculty of Science, University Putra Malaysia, 43400 Serdang, Malaysia; mahnaz@upm.edu.my
[4] Foundation Centre of Agricultural Sciences, University Putra Malaysia, 43400 Serdang, Malaysia
* Correspondence: ali75@uomustansiriyah.edu.iq (A.M.A.A.M.); ekramul@um.edu.my (H.N.M. E.M.); Tel.: +60-1231-3015 (A.M.A.A.M.); +60-3796-72532 (H.N.M.E.M.)

Abstract: The performance of modified electrode of nanocomposite film consisting of polypyrrole-chitosan-titanium dioxide (Ppy-CS-TiO_2) has been explored as non-enzymatic glucose biosensors. The synergy effect of TiO2 nanoparticles and conducting polymer on the current response of electrode resulted in higher sensitivity for nanocomposite modified electrode. The incorporation of TiO_2 nanoparticles in the nanocomposite films were confirmed by XPS spectra. The FESEM and HR-TEM provided more evidences for the presence of TiO_2 in Ppy-CS structure. Glucose biosensing properties were determined by amperommetry and cyclic voltammetry (CV) methods. The interfacial properties of nanocomposite electrodes were studied by electrochemical impedance spectroscopy (EIS). The developed biosensors showed a good sensitivity over the liner range of 1-14 mM with a detection limit of 614 μM for glucose. It also exhibited good selectivity and long term stability with no interference effect. The Ppy-CS-TiO_2 nanocomposites film presented high electron transfer kinetics.

Keywords: nanomaterials; non-enzymatic glucose biosensors; nanocomposites; electrodeposition; titanium dioxide nanocomposite; XPS; EIS.

1. Introduction

The organic–inorganic nanocomposite materials concerned widespread attention because of realizing the combined properties of organic and inorganic components in the same material [1-3]. Conductive polymers and metal oxide nanocomposites with nanoscale dimensions are of special interest for improving the properties of sensors [4-11]. Metals oxides, such as copper oxide (CuO), titanium oxide (TiO_2), iron oxide (Fe_3O_4) are very often recognised as nano oxides in their native or modified forms for the oxidation of glucose [12-14]. Although glucose oxidase (GOx)-based enzymatic biosensors have been usually used for the detection of blood glucose since 1962 [15], however, these enzyme-based sensors show the possible thermal and chemical deformation during fabrication, storage and so on [16,17]. Therefore, non-enzymatic glucose sensors have received great interests particularly through modification of the bare electrode surface with some metal oxide nanoparticles. Modified nanoparticles electrode provides higher surface area improving electron transfer between sensing reaction and electrode [18-21].

Among the metal oxide nanoparticles, titanium dioxide nanoparticles (TiO_2) NPs have been exploited as a potential material for numerous applications because of their unique properties, including high surface area with high catalytic efficiency [22,23]. The importance of these properties is to enhance the interaction between biomolecules and surface of electrode due to higher accessibility

Preprints (www.preprints.org) | NOT PEER-REVIEWED | Posted: 4 April 2017 doi:10.20944/preprints201704.0018.v1

Peer-reviewed version available at Nanomaterials 2017, 7, , 129; doi:10.3390/nano7060129

of target molecules to the sensing area [24-26] thus, newer efforts include metal oxide and conducting polymers as non-enzymatic glucose sensors.

This paper describes the development of nanocomposite films of polypyrrole-chitosan-titanium dioxide nanoparticles (Ppy-CS-TiO_2) on the ITO glass electrode for the detection of glucose, which has not been reported before as non-enzymatic glucose sensors involving TiO_2 as the nanoparticle. The role of TiO_2 as a nanoparticle could enhance the sensing performances such as sensitivity, stability, and selectivity in glucose biosensors by the prepared Ppy-CS-TiO_2 electrode has been reported here.

2. Results and Discussion

The presence of TiO_2 nanoparticles in the nanocomposite films was confirmed by XPS. The XPS wide-scan spectra are presented in Figure 1 (a) and the XPS quantitative elemental analysis of narrow scan is presented in Figure 1 (b), (c), (d) and (e)) respectively. For pyrrole, C ls around (285) eV, N ls around (400) eV, O ls around (531) eV. The main carbon peak at 286.2 eV in chitosan corresponds to carbon bonded with both the hydroxyl group and nitrogen. In the carbon-related spectrum, two other significant peaks were appearing, which can be assigned to carbon to carbon single bonds (284.8) eV and carbonyl groups (approx. 287.8 eV), both are present in the chitosan structure. Moreover, the minor peak in the position of approximately (288.0) eV is noticeable. This peak can be observed as unreacted acidic acid hydroxyl groups (-COO) in Figure 1 (b) [27]. The high-resolution spectrum, however, exposes at least two chemically different nitrogen. The stronger peak at (399.8) eV can be assigned to neutral -N- whereas the higher binding energy peak at (401.0) eV is assigned to the oxidized -N^+ moieties. These values are considered for the conducting of Ppy associated well with the value obtained electrochemically as seen in Figure 1 (d) [28]. The O1s peak for this nanocomposite appears with a split at 530.6 ev in Figure 1 (c) and represents the lattice oxygen. It is shifted slightly compared to database values [29]. It is expected that this shift is caused by the particle diameter of less than 20 nm. Another O1s peak shows at 532.5 eV and is due to the surface oxygen. In this case, the energy is higher compared to the bulk since there are open bonds. Since this material is of nanometer-size, it has a large specific surface area which increases the ratio of surface to bulk oxygen. It has been discussed that the ratio between the two peaks can be correlated to the surface area of the material [30]. In Figure 1 (e), the titanium atom shows two distinct peaks at 458.4 eV for the $Ti2p_{1/2}$ and at 459.2 eV for the $Ti2p_{3/2}$ showing the clear evidence of the element present in the surface of the Ppy-CS-TiO_2 nanocomposite films [31].

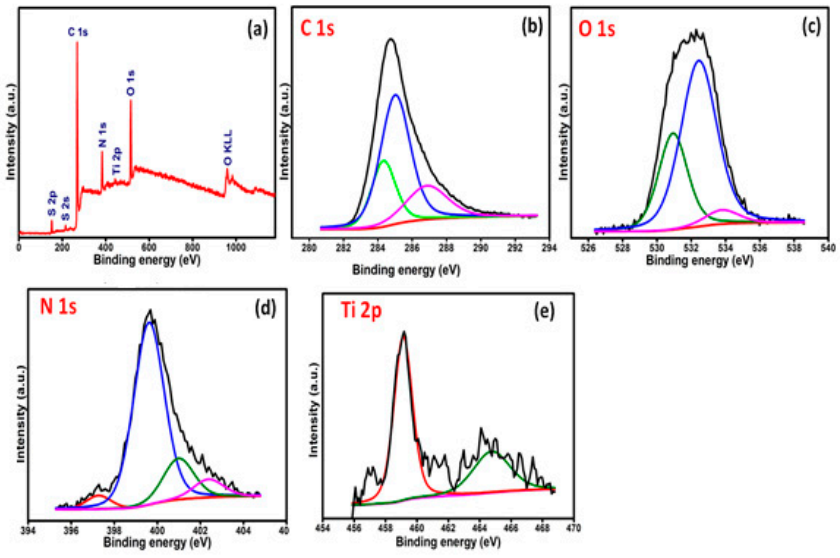

Figure 1. The XPS survey scan (a) and narrow scan (b, c, d, and e) of Ppy-CS-TiO_2 nanocomposite films.

Preprints (www.preprints.org) | NOT PEER-REVIEWED | Posted: 4 April 2017 doi:10.20944/preprints201704.0018.v1

Peer-reviewed version available at Nanomaterials 2017, 7, , 129; doi:10.3390/nano7060129

FE-SEM micrographs confirmed the homogeneous distribution of TiO_2 at the surface of the Ppy-CS-TiO_2 nanocomposites films in Figure 2 (a), which shows the white dots in colour of the nanoparticles of TiO_2. The direct evidence for the incorporation of TiO_2 nanoparticles in Py-CS-TiO_2 nanocomposites was analysed by HR-TEM. The size and dispersion of TiO_2 nanoparticles and Ppy-CS-TiO_2 nanocomposites were measured by HR-TEM in Figure 2 (b and c) respectively. Approximately spherical agglomerated particles were observed for Ppy-CS-TiO_2 nanocomposites and the size ranging from 18 nm to 27 nm. The size of the particles in the nanocomposite was higher than that of the TiO_2 used (>20 nm). The TiO_2 nanoparticles were found to be spherical in shape as seen in Figure 2 (b) and the particle size distribution of TiO_2 nanoparticles was almost uniform. The Ppy-CS-TiO_2 nanocomposites were found to have typical incorporation of TiO_2 into the composite as seen in Figure 2 (c). The dark areas represent the crystalline TiO_2 nanoparticles, while the bright areas represent the amorphous CS, owing to the high electron density of the TiO_2 nanoparticles. The interaction between CS and TiO_2 enhanced the properties of CS-TiO_2 nanocomposites.

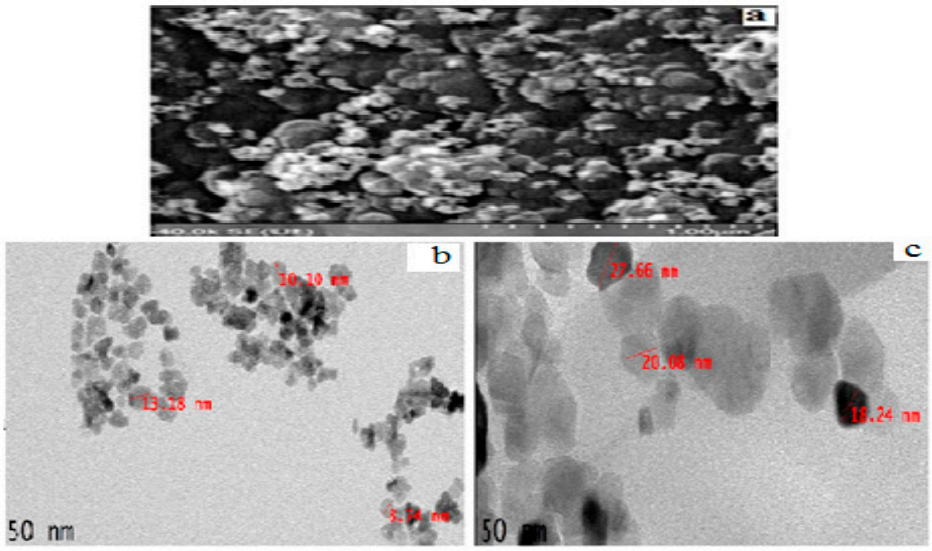

Figure 2. (a) FE-SEM micrograph of Ppy-CS-TiO_2, (b) HR-TEM image of TiO_2 and (c) HR-TEM image Ppy-CS-TiO_2 nanocomposites film.

The glucose sensing performances of Ppy-CS-TiO_2 nanocomposite /ITO was carefully found by cyclic voltammetry (CV) in Figure 3 (a) with and without glucose in alkaline media (0.1M NaOH) at the scan rate of 50 mVs^{-1}. In presence of glucose the peak currents for Ppy-CS-TiO_2 nanocomposite/ITO electrode was observed much higher than without glucose. Thus, Ppy-CS-TiO_2 nanocomposite /ITO is acting as a good glucose sensor due to the glucose oxidation ability of Ppy-CS-TiO_2 nanocomposite.

On the basis of the reported for glucose oxidation and our finding in this study, a possible catalytic of chemical equation for glucose oxidation at Ppy-CS-TiO_2 nanocomposite is proposed as follows:

$$2TiO_2 + \underset{\text{glucose}}{C_6H_{12}O_6} \rightarrow 2TiOOH + \underset{\text{gluconolactone}}{C_6H_{10}O_6} \quad (1)$$

Figure 3 (b) shows typical steady-state amperometric responses of Ppy-CS-TiO_2 nanocomposite /ITO and Ppy-CS /ITO on successively increasing glucose concentration at an applied potential of +0.13 V (vs. Ag/AgCl). The current response of Ppy-CS-TiO_2 /ITO modified electrode toward glucose increased linearly while the Ppy-CS/ITO presented much lower response and only realized a slight increase with the addition of glucose into the cell. The results are consistent with those obtained from cyclic voltammograms. The calibration curve for Ppy-CS-TiO_2 nanocomposite /ITO is presented in the inset of Figure 3 (b). The glucose sensors show linear dependence in the glucose concentration of

Preprints (www.preprints.org) | NOT PEER-REVIEWED | Posted: 4 April 2017 doi:10.20944/preprints201704.0018.v1

Peer-reviewed version available at Nanomaterials 2017, 7, , 129; doi:10.3390/nano7060129

dynamic range of 1 to 14 mM with a correlation coefficient of 0.989, a sensitivity of 0.008 μAcm^{-2} mM^{-1}, and low detection limit (LOD) of 614 μM of (S/N=3). This novel Ppy-CS-TiO_2 nanocomposite /ITO glucose sensor exhibits good sensitivity, low detection limit and fast response time in less than 3 seconds. TiO_2 nanoparticles in PPy-CS-TiO_2 is showing much higher current response compared to the electrode (PPy-CS) without TiO_2 as can be seen in Figure 3 (b) for the amperometric responses to the successive addition of glucose.

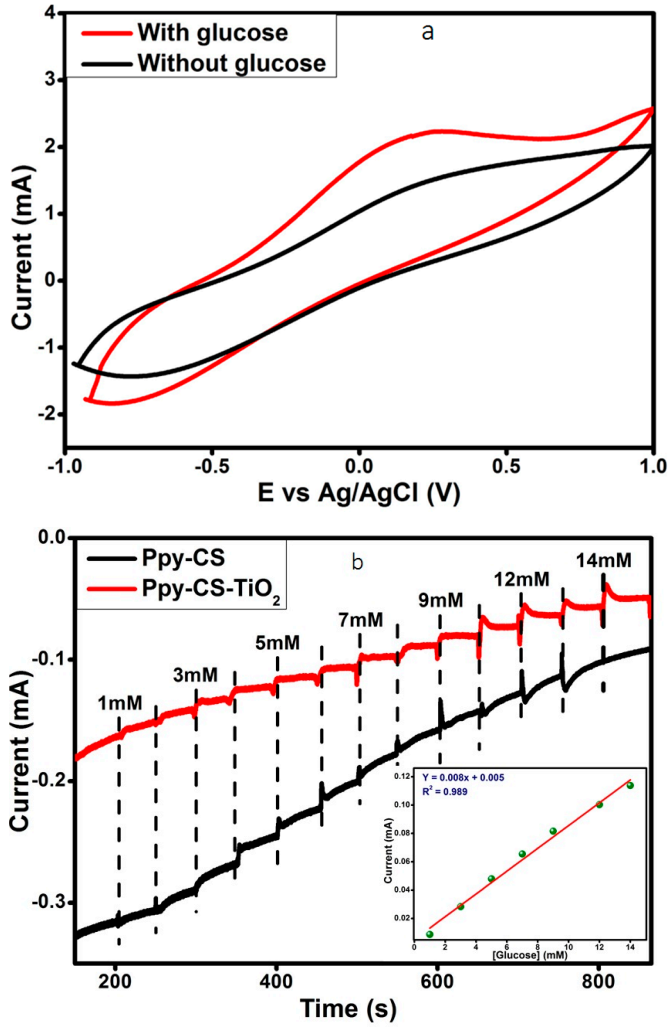

Figure 3. (a) CV responses of Ppy-CS-TiO_2 /ITO in 0.1M NaOH electrolyte with 1mM glucose and without glucose at the scan rate of 50 mVs^{-1}. (b) Amperometric responses to successive addition of glucose concentration in 0.1M NaOH solution at +0.13 V (vs. Ag/AgCl). The inset shows the steady-state calibration curve for the of Ppy-CS-TiO_2 nanocomposite /ITO electrode.

Figure 4 (a) describes the comparison of cyclic voltammetric responses obtained at the bare ITO, Ppy-CS composite and Ppy-CS-TiO_2 nanocomposites for 1 mM $K_3[Fe(CN)_6]$ in 0.1 M KCl at a scan rate of 50 mV s^{-1}. The bare ITO electrode shows a reversible voltammetric characteristic for the one electron redox process of $[Fe(CN)_6]^{3-/4-}$ at a scan rate of 50 mV s^{-1}. The Ppy-CS composite and Ppy-CS-TiO_2 nanocomposite electrodes show in Figure 4 (a) enhanced redox peak currents with a peak to peak separation, when compared to bare ITO. The high conductivity of Ppy facilitated the electron transfer and presented a higher peak current of oxidation and reduction peaks values (480 μA and -500 μA) for the Ppy-CS composite electrode and likewise for the nanocomposite electrode (580 μA and -580 μA). It was found that the nanocomposites containing TiO_2 increase the electrocatalytic activity and appears as a good electrical communicator with the original electrode surface. It was noticeably found that the nanocomposite electrode performs as a new electrode surface; this is due

Preprints (www.preprints.org) | NOT PEER-REVIEWED | Posted: 4 April 2017 doi:10.20944/preprints201704.0018.v1

Peer-reviewed version available at Nanomaterials 2017, 7, , 129; doi:10.3390/nano7060129

to the effect of both TiO_2 and Ppy which increased the electrocatalytic activity and appeared as a good electrical communicator with the original electrode surface.

The interfacial properties of nanocomposite electrodes were studied by electrochemical impedance spectroscopy (EIS) in Figure 4 (b). The Nyquist diagram of the complex impedance shows that the bare ITO electrode has a semicircle-like shape Nyquist plot with a large diameter which recommends the hindrance to the electron-transfer kinetics at the electrode. For Ppy-CS-TiO_2 nanocomposites, no semi-circle was observed which shows the higher electron transfer kinetics. Additionally, the composite and nanocomposite electrodes presented only the linear portion at lower frequencies. This semicircle compared to the other electrodes, which is a result of the large charge-transfer resistance (R_{ct}) at the electrode/electrolyte interface due to the poor electron transfer kinetics. It can obviously be seen that (R_{ct}) decreased for the Ppy-CS composite and Ppy-CS-TiO_2 nanocomposite electrodes, which can be attributed to the presence of high conductive Ppy and catalytically active TiO_2 nanoparticles on the electrode surface. The diffusion-limited process was much more facilitated at the nanocomposite electrodes owing to the conducting properties of Ppy and the large surface area of TiO_2 in the nanocomposites.

The conducting nature of Ppy in both the composite and nanocomposite electrode facilitates the peak shifting in the Bode plot showed in Figure 4 (c). The Bode impedance plot of the nanocomposite electrode presented a lesser log Z value in a low frequency range of 1–100 Hz when compared to the composite electrodes.

In Figure 4 (d), the Bode-phase plots of the nanocomposite electrodes were collected in the frequency range of 0.01–10000 Hz. The phase peaks appeared at a frequency range of 100–10000 Hz which corresponds to the charge-transfer resistance of the nanocomposite electrodes. The shifting of peaks toward the low frequency region of 1–0.01 Hz for composite and nanocomposite electrodes indicates the fast electron-transfer behaviour of the nanocomposites. A perfect linear portion was observed at lower frequencies for the nanocomposite electrode compared to the other electrodes. These results indicate that the Ppy-CS-TiO_2 nanocomposite was successfully designed and it facilitated a diffusion-limited process at the electrode-solution interface.

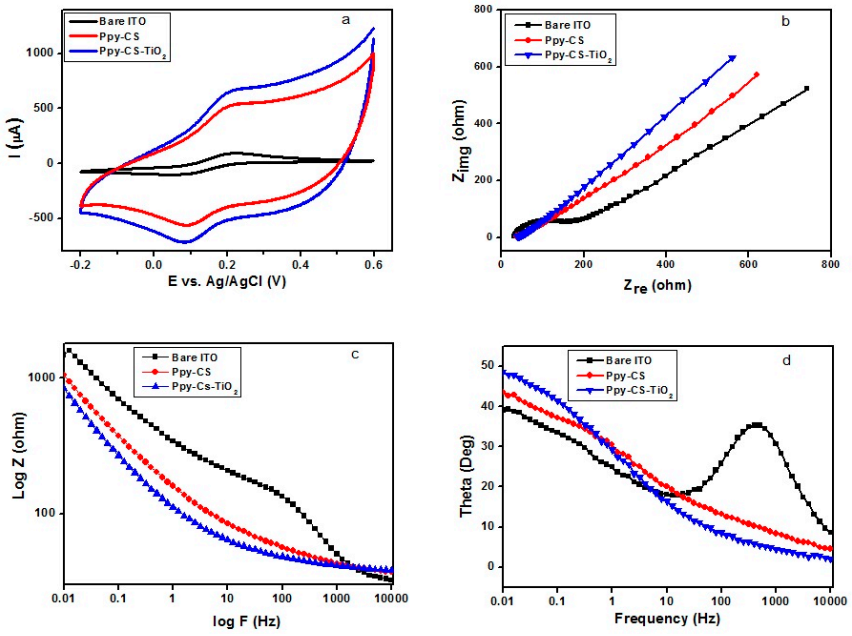

Figure 4. (a) Cyclic voltammograms obtained for bare ITO, Ppy-CS composite and Ppy-CS-TiO_2 nanocomposites (b) Nyquist plots, (c) Bode impedance phase plots of log z, (d) Bode phase plots, for 1 mM $K_3[Fe(CN)_6]$ in 0.1 MKCl at a scan rate of 50 mVs^{-1} vs (Ag/AgCl).

Preprints (www.preprints.org) | NOT PEER-REVIEWED | Posted: 4 April 2017 doi:10.20944/preprints201704.0018.v1

Peer-reviewed version available at Nanomaterials 2017, 7, , 129; doi:10.3390/nano7060129

The stability of the developed sensor was investigated by measuring its current response for glucose for 14 days. The prepared Ppy-CS-TiO_2 nanocomposite films on ITO was used to record the amparometric response for 1mM glucose with a frequency of 2 days. Figure 5 represented stability of Ppy-CS-TiO_2/ ITO modified electrode over 14 days. I_0 is the current response of fresh sensor and I_{14} is the current response after 14days storage as shown in Figure 5. During the first 6 days, the current response did not change in a noticeable way. However, on the 14th day (last day), the current response still remained above 88 % of its initial response, revealing the excellent stability of the non-enzymatic glucose sensor.

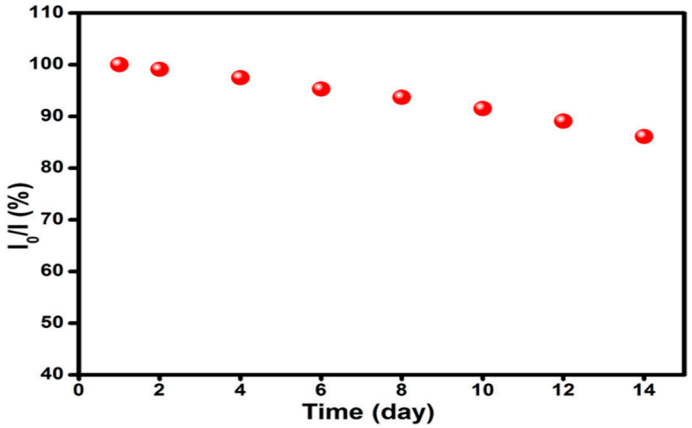

Figure 5. Stability of the sensor stored at ambient conditions over 14 days in 0.1 M NaOH glucose at potential of 0.13 V (vs. Ag/AgCl).

The selectivity of the Ppy-CS-TiO_2 nanocomposite /ITO for the detection of glucose was examined by injecting three different interfering biomolecules, namely, (UA), (AA) and (CH) in the evenly stirred 0.1 M NaOH solution containing glucose. Figure 6 depicts the recorded amperometric responses for the consecutive additions of glucose and the interfering biomolecules. First, the successive injections of glucose (each time, 1 mM) were used to record the current response for two injections after every 50 sec. The clear response towards detection was observed. No response was observed after that the consecutive injections of UA, AA and cholesterol (each time, 0.1 mM) in the same stirred solution. Later glucose was added by three injections (each time, 1 mM) and the current response was observed. It was found that, the addition of interfering biomolecules did not contribute significant changes on current response contrary to the glucose solution which represented a high response for each injection. These results revealed that the present sensor possesses a good selectivity and sensitivity towards the detection of glucose even in the presence of common physiological interfering biomolecules.

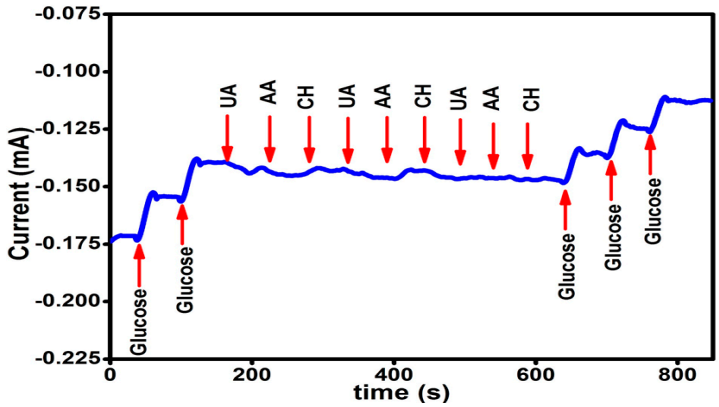

Figure 6. Amperometric responses obtained at successive addition of glucose and each of uric acid, ascorbic acid and cholesterol in 0.1 M NaOH solution at +0.13 V (vs. Ag/AgCl) with regular interval of 50 s.

Preprints (www.preprints.org) | NOT PEER-REVIEWED | Posted: 4 April 2017 doi:10.20944/preprints201704.0018.v1

Peer-reviewed version available at Nanomaterials 2017, 7, , 129; doi:10.3390/nano7060129

3. Materials and Methods

Chitosan, was purchased from (ACROS Organics), New Jersey, USA. TiO_2 Np >20 nm, D (+) glucose sodium, para toluene sulfonate (*P*-TS), ascorbic acid (AA), uric acid (UA) and cholesterol (CH) were all purchased from Sigma–Aldrich. Acetic acid, sodium hydroxide and freshly distilled pyrrole 99% were provided by Merck. Indium tin oxide (ITO) glass electrode was purchased from (Fluka, Japan). A stock solution of D (+) glucose was prepared (1M) and left overnight for studying the sensing performance of the modified electrode. A stock solution of NaOH (0.1 M) was prepared using distilled water. A stock solution was prepared containing potassium ferricyanide ($1x10^{-3}$) M $K_3[Fe(CN)_6]$ in potassium chloride (0.1) M KCl.

3.1 Instrument

Field emission scanning electron microscope (FESEM, Hitachi Brand, Model SU 8220) and high-resolution transmission electron microscope (HRTEM) (Tecnai model G2-F20)-Twin manufacture (FEI, USA) were used for the investigation of the morphology and structural properties of the deposited nanocomposite films. The presence of the nanoparticles in the prepared films was determined by X-ray photoelectron spectroscopy (XPS) brand (ULVAC-PHI Quantera II (Ulvac-PHI, INC). All electrochemical measurements were performed using a computerized potentiostat Instrument, made by Digi-ivy, Inc.(USA). A conventional three-electrode system comprising of an ITO glass electrode, graphite rode and Ag/AgCl were used as working electrode, counter electrode and reference electrode, respectively.

3.2 Preparation of Ppy-CS -TiO_2 NP/ ITO nanocomposite films

TiO_2 Np were dispersed into 25 mL of CS (50 mg/mL) solution under continuous stirring at room temperature followed by ultrasonicating for 2 h to obtain a viscous solution of CS with uniformly dispersed TiO_2 Np. Later certain amount of pyrrole and *p*-TS as a dopant were added to the CS and TiO_2 dispersion and stirred for 5 min. The prepared dispersion of Ppy-CS-TiO_2 was used for the electrochemical deposition of the film on ITO glass electrode by cyclic voltammetry scanning ranging from -1V to +1.2 V (vs. Ag/AgCl) with a scan rate of 50 mV/s using the three-electrode system. The Ppy-CS-TiO_2 nanocomposite films were then washed repeatedly with distilled water to remove any unbound particles and later dried at room temperature. The prepared films were characterized and subjected to electrochemical oxidation of glucose.

3.3 Mechanism for the formation of Ppy-CS-TiO_2 on ITO

In this study, cyclic voltammetry was used for the electrochemical deposition of conducting polymer nanocomposite films on ITO glass electrode where all the components like the monomer, the dopant, chitosan, and the nanoparticle were dissolved in the solvent in the electrochemical cell as seen in Figure 7.

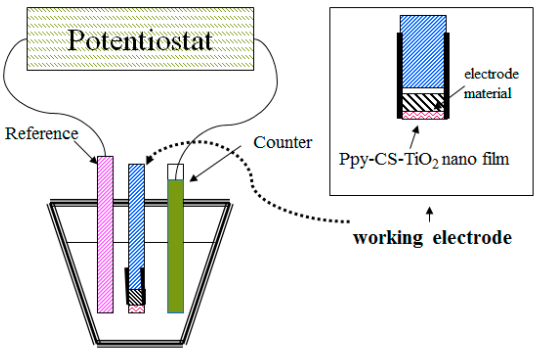

Figure 7. The electrochemical cell of Ppy- CS-TiO_2 film preparation

Preprints (www.preprints.org) | NOT PEER-REVIEWED | Posted: 4 April 2017 doi:10.20944/preprints201704.0018.v1

Peer-reviewed version available at Nanomaterials 2017, 7, , 129; doi:10.3390/nano7060129

During this one-step, electrochemical formation of CS–PPy–TiO_2 nanocomposite films, polypyrrole is linked with CS-TiO_2 through hydrogen bonding and titanium-nitrogen ligand formation. The CS-TiO_2 are linked with hydrogen bonding during ultra-sonication in the preparatory stage as shown in Figure 8.

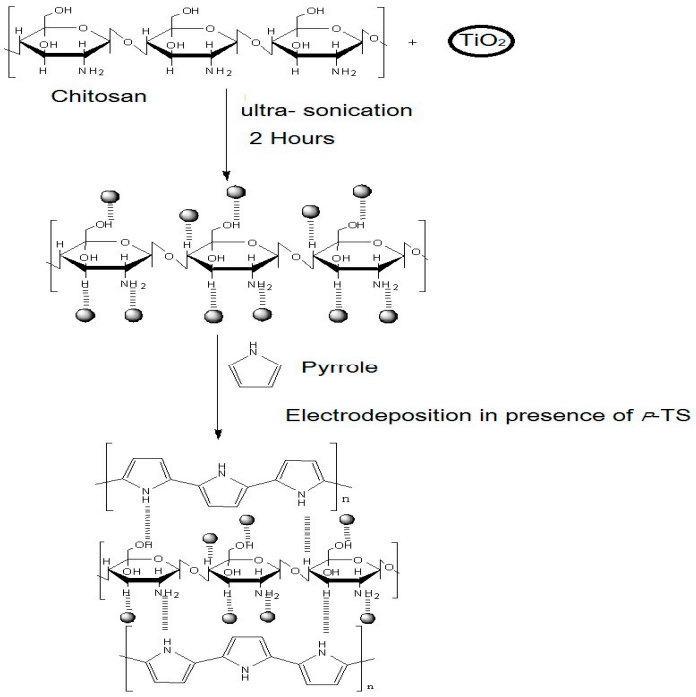

Figure 8. The mechanism of Ppy- CS-TiO_2 film electrodeposition.

4. Conclusions

We wish to report on the successful preparation of PPy-CS-TiO_2 nanocomposite films on ITO glass electrode as non-enzymatic glucose biosensors. The electrochemically prepared nanocomposite films (PPy-CS-TiO_2) exhibited an excellent electrocatalysis towards glucose oxidation in alkaline media. TiO_2 as a nanomaterial played a vital role in glucose oxidation together with polypyrrole and chitosan as has been observed in this study. The nanocomposite films showed a low detection limit, wide linear range, fast response time, high current for glucose oxidation with good stability. EIS study shows the lowest charge transfer resistance for the prepared (PPy-CS-TiO_2) nanocomposite films. As a glucose sensor, the prepared (PPy-CS-TiO_2) nanocomposite electrode is immune to other biomolecules such as uric acid, ascorbic acid and cholesterol. Considering the low-cost, facile and controllable method for the preparation of (PPy-CS-TiO_2) nanocomposite films and improved electrocatalytic activity toward glucose oxidation, the future of this non-enzymatic glucose sensor looks bright.

Acknowledgments: The authors would like to acknowledge the financial supports from the Ministry of Higher Education, Malaysia for the Fundamental Research Grant Scheme (FRGS) (Project No. FP034-2013A) and the University of Malaya Postgraduate Research Grant (PPP) (Project No: PG111-2013A). The author would like also to thank AL-Mustansiriyah University (www.uomustansiriyah.edu.iq) for its support in the present work.

Author Contributions: Habibun Nabi Muhammad Ekramul Mahmud organized and supervised this work; Ali M.A. Abdul Amir AL-Mokaram wrote the article and analyzed part of the data; Rosiyah Yahya supported and analyzed part of the data; Mahnaz M Abdi performed the data analyses.

Conflicts of Interest: The authors declare no conflicts of interest.

Preprints (www.preprints.org) | NOT PEER-REVIEWED | Posted: 4 April 2017 doi:10.20944/preprints201704.0018.v1

Peer-reviewed version available at Nanomaterials 2017, 7, , 129; doi:10.3390/nano7060129

References

1. Sanchez, C., Soler-Illia, G. D. A., Ribot, F., Lalot, T., Mayer, C. R., & Cabuil, V. Designed hybrid organic-inorganic nanocomposites from functional nanobuilding blocks. *Chem. Mat*. **2001**, 13(10), 3061-3083.
2. Mitzi, D. B. Thin-film deposition of organic-inorganic hybrid materials. *Chem. Mat*. **2001**, 13(10), 3283-3298.
3. Gómez-Romero, P., Chojak, M., Cuentas-Gallegos, K., Asensio, J. A., Kulesza, P. J., Casañ-Pastor, N., & Lira-Cantú, M. Hybrid organic–inorganic nanocomposite materials for application in solid state electrochemical supercapacitors. *Electrochem. Commun*. **2003**, 5(2), 149-153.
4. Coronado, E., Galán-Mascarós, J. R., Gómez-García, C. J., & Laukhin, V. Coexistence of ferromagnetism and metallic conductivity in a molecule-based layered compound. *Nature*. **2000**, 408(6811),447-449.
5. Sidorov, S. N., Volkov, I. V., Davankov, V. A., Tsyurupa, M. P., Valetsky, P. M., Bronstein, L. M., & Lakina, N. V. Platinum-containing hyper-cross-linked polystyrene as a modifier-free selective catalyst for L-sorbose oxidation. *J. Am. Chem. Soc*. **2001**, 123(43), 10502-10510.
6. Merkel, T. C., Freeman, B. D., Spontak, R. J., He, Z., Pinnau, I., Meakin, P., & Hill, A. JUltrapermeable, reverse-selective nanocomposite membranes. *Science*. **2002**, 296 (5567), 519-522.
7. Wu, H., Wang, J., Kang, X., Wang, C., Wang, D., Liu, J., & Lin, Y. Glucose biosensor based on immobilization of glucose oxidase in platinum nanoparticles/graphene/chitosan nanocomposite film. *Talanta*. **2009**, 80(1), 403-406.
8. Tsai, Y. C., Li, S. C., & Liao, S. W. Electrodeposition of polypyrrole–multiwalled carbon nanotube–glucose oxidase nanobiocomposite film for the detection of glucose. *Biosens. Bioelectron*. **2006**, 22(4), 495-500.
9. Butterworth, M. D., Corradi, R., Johal, J., Lascelles, S. F., Maeda, S., & Armes, S. P. Zeta potential measurements on conducting polymer-inorganic oxide nanocomposite particles. *J. Colloid Interface Sci*. **1995**, 174(2), 510-517.
10. Hajji, P., David, L., Gerard, J. F., Pascault, J. P., & Vigier, G. Synthesis, structure, and morphology of polymer–silica hybrid nanocomposites based on hydroxyethyl methacrylate. *J. Polym. Sci. Pt. B-Polym. Phys*. **1999**, 37(22), 3172-3187.
11. Yoon, H. Current trends in sensors based on conducting polymer nanomaterials. *Nanomaterials*. **2013**, *3*(3), 524-549.
12. Zhang, J., Ma, J., Zhang, S., Wang, W., & Chen, Z. A highly sensitive nonenzymatic glucose sensor based on CuO nanoparticles decorated carbon spheres. *Sens. Actuator B-Chem*. **2015** ,211, 385-391.
13. Bao, S. J., Li, C. M., Zang, J. F., Cui, X. Q., Qiao, Y., & Guo, J. New nanostructured TiO2 for direct electrochemistry and glucose sensor applications. *Adv. Funct. Mater*. **2008**, 18(4), 591-599.
14. Wei, H., & Wang, E. Fe3O4 magnetic nanoparticles as peroxidase mimetics and their applications in H2O2 and glucose detection. *Anal. Chem. **2008***, 80(6), 2250-2254.
15. Wang, L., Gao, X., Jin, L., Wu, Q., Chen, Z., & Lin, X. Amperometric glucose biosensor based on silver nanowires and glucose oxidase. *Sens. Actuator B*-Chem.**2013**, 176, 9-14.
16. Ramanavicius, A., Kausaite, A., Ramanaviciene, A., Acaite, J., & Malinauskas, A. Redox enzyme–glucose oxidase–initiated synthesis of polypyrrole. *Synth. Met*. **2006**, 156(5), 409-413.
17. Welch, C. M., & Compton, R. G. The use of nanoparticles in electroanalysis: a review. *Anal. Bioanal. Chem*. **2006**, 384(3), 601-619.
18. Huang, J., Dong, Z., Li, Y., Li, J., Wang, J., Yang, H., & Li, R. High performance non-enzymatic glucose biosensor based on copper nanowires–carbon nanotubes hybrid for intracellular glucose study. *Sens. Actuator B-Chem*.**2013**, 182, 618-624.
19. Xiao, X., Li, H., Pan, Y., & Si, P. Non-enzymatic glucose sensors based on controllable nanporous gold/copper oxide nanohybrids. *Talanta*. **2014**, 125, 366-371.
20. Zaidi, S. A., & Shin, J. H. Recent developments in nanostructure based electrochemical glucose sensors. *Talanta*. **2016**, 149, 30-42.
21. Guan, P., Li, Y., Zhang, J., & Li, W. Non-Enzymatic Glucose Biosensor Based on CuO-Decorated CeO2 Nanoparticles. *Nanomaterials*. **2016**, *6*(9), 159.
22. Yang, Q., Long, M., Tan, L., Zhang, Y., Ouyang, J., Liu, P., & Tang, A. Helical TiO2 nanotube arrays modified by Cu–Cu2O with ultrahigh sensitivity for the nonenzymatic electro-oxidation of glucose. *ACS Appl. Mater. Interfaces*. **2015**, 7(23), 12719-12730.
23. He, M. Q., Bao, L. L., Sun, K. Y., Zhao, D. X., Li, W. B., Xia, J. X., & Li, H. M. Synthesis of molecularly imprinted polypyrrole/titanium dioxide nanocomposites and its selective photocatalytic degradation of rhodamine B under visible light irradiation. ***Express Polym Lett***. **2014**, 8(11),850–861.

Preprints (www.preprints.org) | NOT PEER-REVIEWED | Posted: 4 April 2017 doi:10.20944/preprints201704.0018.v1

Peer-reviewed version available at Nanomaterials 2017, 7, , 129; doi:10.3390/nano7060129

24. Si, P., Ding, S., Yuan, J., Lou, X. W., & Kim, D. H. Hierarchically structured one-dimensional TiO2 for protein immobilization, direct electrochemistry, and mediator-free glucose sensing. *ACS nano*. **2011**, 5(9), 7617-7626.
25. Bai, J., & Zhou, B. Titanium dioxide nanomaterials for sensor applications. *Chem. Rev*. **2014**, 114(19), 10131-10176.
26. Chen, J., Xu, L., Xing, R., Song, J., Song, H., Liu, D., & Zhou, J. Electrospun three-dimensional porous CuO/TiO2 hierarchical nanocomposites electrode for nonenzymatic glucose biosensing. *Electrochem. Commun*. **2012**, 20, 75-78.
27. Lawrie, G., Keen, I., Drew, B., Chandler-Temple, A., Rintoul, L., Fredericks, P., & Grøndahl, L. Interactions between alginate and chitosan biopolymers characterized using FTIR and XPS. *Biomacromolecules*. **2007**, 8(8), 2533-2541.
28. Kang, E. T., Neoh, K. G., & Tan, K. L. X-ray photoelectron spectroscopic studies of electroactive polymers. In *Polymer Characteristics*, Springer Berlin Heidelberg, Germany ,1993; Volume 106, pp.135-190.
29. Wagner, C. D., Naumkin, A. V., Kraut-Vass, A., Allison, J. W., Powell, C. J., & Rumble Jr, J. R. NIST X-ray Photoelectron Spectroscopy Database, *NIST Standard Reference Database.* 2003, 20, Version 3.4 (Web Version).
30. Jensen, H., Soloviev, A., Li, Z., & Søgaard, E. G. XPS and FTIR investigation of the surface properties of different prepared titania nano-powders. *Appl. Surf. Sci.***2005**, 246(1), 239-249.
31. Sathe, A., Peck, M. A., Balasanthiran, C., Langell, M. A., Rioux, R. M., & Hoefelmeyer, J. D. X-ray photoelectron spectroscopy of transition metal ions attached to the surface of rod-shape anatase TiO2 nanocrystals. *Inorg. Chim. Acta*. **2014**, 422, 8-13.

© 2017 by the authors. Licensee *Preprints*, Basel, Switzerland. This article is an open access article distributed under the terms and conditions of the Creative Commons by Attribution (CC-BY) license (http://creativecommons.org/licenses/by/4.0/).